Proceedings of the 9ICEG
9th International Congress on Environmental Geotechnics
25-28 June, 2023 | Chania, Greece
© Authors: All rights reserved, 2023
https://doi.org/10.53243/ICEG2023-98

Analytical interpretation of swelling behavior of air-dried bentonite using double structure model based on mineral crystal phenomena

H. Kyokawa[1], Y. Muto[2] and H. Wang[3]

[1]*Associate Professor, Nagoya Institute of Technology, Nagoya, Japan. Email: kyokawa@nitech.ac.jp*

[2]*Graduate Student, University of Tokyo, Tokyo, Japan*

[3]*Associsate Professor, Waseda University, Tokyo, Japan*

ABSTRACT

Bentonite, a well-known expansive soil, is intended to use as a sealing and/or buffer materials surrounding radioactive waste in waste disposal facilities, because of its hydro-mechano-chemical characteristics, such as self-healing properties, low permeability, and radionuclide absorptivity. In particular, many studies on its swelling characteristics have been conducted, and it has been revealed that the microscopic swelling characteristic of expansive mineral crystals (montmorillonite) governs the macroscopic behavior. However, few suitable constitutive models quantitatively describe the interaction between the microscopic and macroscopic swelling behaviors of expansive soils. Focusing on the hydro-chemical phenomena on the surface of mineral crystal that characterize expansive soils, the author proposed a double-structure model that represents the macroscopic behavior of the expansive soils as a combination of the soil skeleton behavior and the interlaminar behaviors of clay mineral crystals. In this study, by applying this model to the swelling behavior of Kunigel-V1 bentonite at water contents ranging from the dry condition to the fully saturated condition, the swelling behavior of bentonite was interpreted from the double-void structure perspective.

Keywords: bentonite, constitutive model, swelling, mineral crystal, HMC coupling

1 INTRODUCTION

Numerous constitutive models of expansive soils have been proposed with the objective of predicting the conduct of bentonites as buffering materials in waste disposal facilities. Analyzing detailed experimental data, phenomenological models, which directly associate the macroscopic behavior with stress and suction as general (unsaturated) soil mechanics, has been developed (e.g., Millard et al., 2016; Liu et al., 2021; Sun et al., 2022). The double structure framework (Gens and Alonso, 1992), in which soils are regarded as composition of a macrostructure and a microstructure, is one representative framework for the modeling of expansive soils. Based on this framework, several improved and extended models to capture complex THMC behaviors of expansive soils have been proposed (e.g., Alonso et al., 1999; Guimarães et al., 2013; Sànchez et al., 2016; Mašín, 2017; Yie and Vanapalli, 2022; Rosone and Ferrari, 2022). Recently, the models incorporating the chemical potential, which would be an essential factor to comprehensively understand osmotic phenomena of expansive soil, has also been proposed (e.g., Tuttolomondo et al., 2021; Navarro, et al., 2022). On the other hand, it is known that the typical behavior of expansive soils, especially swelling behavior, is caused by the nanoscale electro-chemical phenomena on the surface of the main constituent mineral. However, few models have been developed to describe the behavior of bentonite from the microstructural mineral crystal point of view.

Focusing on the hydro-mechano-chemical phenomena on the surface of mineral crystal, Kyokawa (2021) proposed a double-structure model that represents the macroscopic behavior of expansive soils as a combination of the soil skeleton and interlaminar behaviors of mineral crystals. This model was validated by simulating element tests on wetted (unsaturated) and heavily compacted bentonite. In this study, this model is extended to consider a general multi-cation condition, namely the cation exchange. Moreover, the simulation of the wetting process of Kunigel-V1 bentonite from the air-dried state to the fully saturated state with different cation conditions is conducted. Kunigel-V1 bentonite is one of the

most popular sodium-type bentonites in Japan, and there are enough previous studies for the model validation. By fitting the microscopic behavior, such as the variation in the basal spacing (the interlaminar distance plus thickness of crystal), and the macroscopic stress-strain behavior, the model can comprehensively describe the swelling behavior of Kunigel-V1 bentonite under different pore fluid conditions.

2 OUTLINE OF CONSTITUTIVE MODEL FOR EXPANSIVE SOIL

2.1 Double structure modeling of unsaturated expansive soil

In this study, the swelling pressure tests on Kunigel-V1 bentonite with different ion conditions are simulated using a constitutive model. This chapter briefly explains the constitutive model of an expansive soil based on the double structure framework (Kyokawa, 2021), and its extension to consider the multi-cations condition. The strain of the expansive soil is composed of the soil skeleton strain $\varepsilon_{ij}^{\mathrm{ss}}$ and the interlaminar strain $\varepsilon_{ij}^{\mathrm{il}}$ as

$$\varepsilon_{ij} = \varepsilon_{ij}^{\mathrm{ss}} + \varepsilon_{ij}^{\mathrm{il}} = \varepsilon_{ij}^{\mathrm{ss}} - \theta^{*}\,(d - d_0)/(3d_0)\,\delta_{ij} \;\text{ where }\; \theta^{*} = e_0^{\mathrm{il}}/\left(1 + e_0^{\mathrm{ss}} + e_0^{\mathrm{il}}\right) \tag{1}$$

where d is the (half) interlaminar distance shown in Figure 1, e_0^{il} is the initial interlaminar void ratio and e_0^{ss} is the soil skeleton void ratio. Considering that at least one water layer is constituted in the interlaminar space, namely the interlaminar void is always saturated, the degree of saturation is given by

$$S_{\mathrm{r}} = \left(e^{\mathrm{il}}/e^{\mathrm{ss}} + S_{\mathrm{r}}^{\mathrm{ss}}\right)/\left(e^{\mathrm{il}}/e^{\mathrm{ss}} + 1\right) \tag{2}$$

where $S_{\mathrm{r}}^{\mathrm{ss}}$ is the soil skeleton degree of saturation. Assuming that it is governed by suction, it can be expressed using a classical soil-water characteristic curve model, which is the van Genuchten equation (1980) in this study.

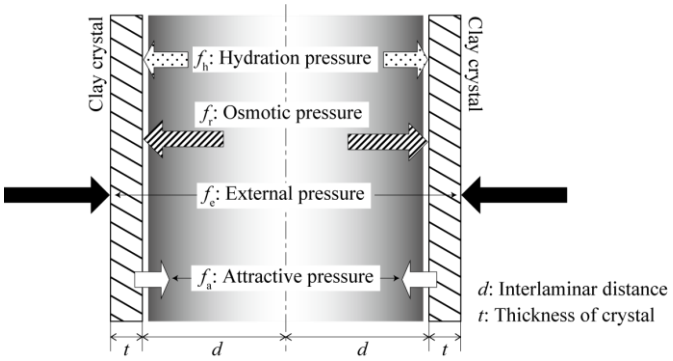


Figure 1. *Layered-clay mineral crystal model and the interlaminar forces*

2.2 Modeling of the interlaminar behavior and cation exchange

It is assumed that the hydro-mechano-chemical forces acting on adjacent crystals are balanced. This equilibrium is schematically depicted in Figure 1 and is formulated as

$$F^{*}\left(d, c_i, \sigma"_{ij}, S_{\mathrm{r}}^{\mathrm{ss}}, EXC_i\right) = -f_{\mathrm{h}}(d, S_{\mathrm{r}}^{\mathrm{ss}}) - f_{\mathrm{o}}(d, c_i, S_{\mathrm{r}}^{\mathrm{ss}}, EXC_i) + f_{\mathrm{a}}(d) + f_{\mathrm{e}}\left(\sigma"_{ij}\right) = 0 \tag{3}$$

where f_{h} is the hydration pressure, f_{o} is the osmotic pressure, f_{a} is the van der Waals pressure, f_{e} is the external pressure, c_i is the concentration of the i-cation, EXC_i is the exchange capacity of the i-cation, and $\sigma"_{ij}$ is the effective stress defined later in this paper. Here, the repulsive pressures (f_{h} and f_{o}) significantly affect the swelling behavior. Refer to Kyokawa (2021) for the details of each formulation.

The osmotic pressure is expressed by the following equation to reflect the multi-cation condition:

$$f_{\mathrm{o}} = S_{\mathrm{r}}^{\mathrm{ss}} \sum_{i=\mathrm{Na}^{+},\ \mathrm{Ca}^{2+},\ldots} \left(x_i \cdot f'_{\mathrm{o}i}(c_i, d)\right) \;\text{ where } x_i = EXC_i/CEC \text{ and } \sum_{i=\mathrm{Na}^{+},\ \mathrm{Ca}^{2+},\ldots} x_i = 1 \tag{4}$$

osmotic pressure for the i-cation, which was originally proposed by Komine and Ogata (1996). It should be noted that the influence of anion on osmotic pressure is not considered in this mode, and it will be a future work. The influence of cation exchange is newly considered to adapt the model (Kyokawa, 2021) to a general multi-cation condition. By following a previous study (Momii et al., 1997), the adsorption ratio x_i is evaluated under multi-cation conditions. Considering four cations (Na^+, Ca^{2+}, K^+ and Mg^{2+}), the following chemical equilibria between the pore water and the adsorption site X, which is a mineral surface, are assumed as

$$2Na^+ + CaX_2 = Ca^{2+} + 2NaX, \quad Na^+ + KX = K + NaX, \quad 2Na^+ + MgX_2 = Mg^{2+} + 2NaX \tag{5}$$

Using the Gaines–Thomas selectivity coefficient, the following law of mass actions based on sodium ion is derived as

$$K_{\mathrm{Na}/j} = (x_{\mathrm{Na}}/a_{\mathrm{Na}})^{v_j} * \left(a_j/x_j\right) \text{ where } j = \mathrm{Ca}, \mathrm{K} \text{ and } \mathrm{Mg} \tag{6}$$

where $K_{\mathrm{Na}/j}$ is the selectivity coefficient of the j-cation against Na^+, and a_j is the activity of the j-cation. Supplied that the sum of the adsorption ratios is equal to one, the adsorption ratio of the i-cation can be calculated.

2.3 Modeling of the soil skeleton behavior

The soil skeleton behavior is influenced by the arrangement and orientation of particles or crystals, and is directly related to the mechanical deformation and strength characteristics of geomaterials. The soil skeleton behavior of unsaturated expansive soil is modeled by Kikumoto et al. (2010) and Komolvilas et al.(2022). The effective stress is the Bishop's effective stress $\sigma"_{ij}$, and the effective stress parameter χ is the soil skeleton degree of saturation $S_{\mathrm{r}}^{\mathrm{ss}}$. Using the soil skeleton degree of saturation $S_{\mathrm{r}}^{\mathrm{ss}}$ instead of the degree of saturation S_{r} means that the surface tension of water between the soil particles or crystals sustains the soil skeleton.

$$\sigma"_{ij} = \left(\sigma_{ij} - u^{\mathrm{a}}\delta_{ij}\right) + \chi(u^{\mathrm{w}} - u^{\mathrm{a}})\delta_{ij} = \sigma_{ij}^{\mathrm{net}} + \chi s = \sigma_{ij}^{\mathrm{net}} + S_{\mathrm{r}}^{\mathrm{ss}} s \tag{7}$$

where u^{w} is the pore water pressure, u^{a} is the pore air pressure and s is the suction.

In addition to the general elastoplastic constitutive model for soils, the soil skeleton strain comprises the elastic and plastic components, and Hooke's law is assumed for elastic strain. For plastic strain, the yield surface based on the modified Cam clay model is given by

$$f = \ln\frac{p"}{p"_0} + \ln\left(\frac{M^2+\eta"^2}{M^2}\right) - \frac{1}{\mathrm{C_p}}\varepsilon_{\mathrm{v}}^{\mathrm{p\,ss}} - \frac{1}{\mathrm{C_p}}\left(\frac{\psi-\psi_0}{1+e_0}\right) + \frac{1}{\mathrm{C_p}}\left(\frac{\rho-\rho_0}{1+e_0}\right) = 0 \text{ where } \mathrm{C_p} = \frac{\lambda-\kappa}{1+e_0} \text{ and } \eta" = \frac{q}{p"} \tag{8}$$

where $\varepsilon_{\mathrm{v}}^{\mathrm{p\,ss}}$ is the plastic volumetric strain of the soil skeleton and it is the hardening parameter. The state variable ψ is added to capture the unsaturated soil behaviors, particularly the wetting collapse.

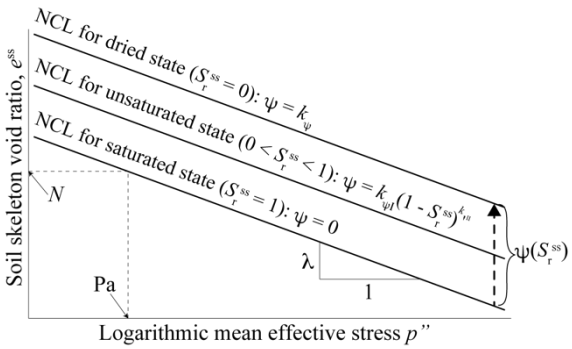


Figure 2. *State variable ψ considering the effect of unsaturated state*

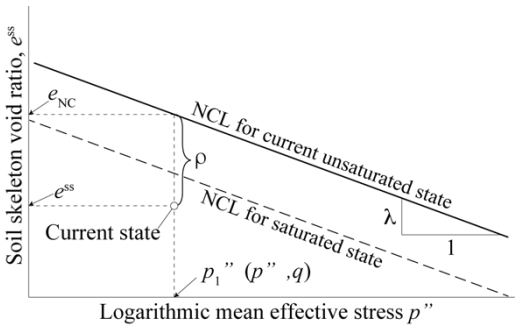


Figure 3. *State variable ρ considering the effect of overconsolidated state*

Figure 2 shows the movement of the normally consolidated line according to the soil skeleton degree of saturation. Moreover, state variable ρ represents the vertical distance between the current void ratio and the normally consolidated line (Figure 3). The concept of the state variable ρ is equal to the over-consolidation ratio. Both state variables and their evolution rules contribute to the reproduction of a smooth constitutive relationship during the hydro-mechano-chemical process.

3 SIMULATIONS OF SWELLING TEST ON AIR-DRIED BENTONITE

3.1 Constitutive parameters

A series of swelling tests on the air-dried Kunigel-V1 bentonites were simulated by the proposed model. The constitutive parameters are listed in Table 1, and they can be classified into five groups: soil skeleton behavior, soil water characteristic (van Gehuchten model), clay mineral and water specifications, physical constants, and initial conditions.

Table 1. *Constitutive parameters*

Parameters for soil skeleton behavior			
λ	Compression index	-	0.130
κ	Swelling index	-	0.040
M	Critical stress ratio	-	0.49
ν_e	Poisson's ratio	-	0.42
e_{NC}	Reference void ratio on NCL at p'' = Pa	-	0.60
Pa	Reference confining pressure	kPa	700
a	Effect of density	-	300
k_I	Effect of unsaturated state	-	1.6
k_{II}	Effect of unsaturated state	-	8.0
κ	Swelling index	-	0.040
M	Critical stress ratio	-	0.49
ν_e	Poisson's ratio	-	0.42
e_{NC}	Reference void ratio on NCL at p'' = Pa	-	0.60
Pa	Reference confining pressure	kPa	700
a	Effect of density	-	300

Parameters of WRC model			
α	VG model parameter	1/kPa	0.0014
m	VG model parameter	-	0.4
n	VG model parameter	-	1.667

Void ratios for double structure			
e_0	Initial void ratio	-	Depending on ρ_{d0}
$e^{ss}{}_0$	Initial soil skeleton ratio	-	$e_0 - e^{il}{}_0$
$e^{il}{}_0$	Initial interlaminar void ratio	-	0.05

Physical constants			
A_h	Hamaker constant	J	2.200E-20
k	Boltzmann constant	J/K	1.380E-23
e'	Electronic charge	C	1.609E-19

Bentonite specifications			
t	Thickness of crystal	m	9.60E-10
S	Specific surface area of crystal	m^2/g	388.8
CEC	Cation exchange capacity	mEq/g	0.732
$K_{Na/Na}$	Cation selectivity against Na^+- Na^+	-	1.00
$K_{Na/Ca}$	Cation selectivity against Na^+- Ca^{2+}	-	0.14
$K_{Na/K}$	Cation selectivity against Na^+- K^+	-	0.12
$K_{Na/Mg}$	Cation selectivity against Na^+- Mg^{2+}	-	0.21
W_{max}	Parameter for the hydration force	MJ/m^2	4.00E-03
W_{min}	Parameter for the hydration force	MJ/m^2	8.00E-05
χ_0	Parameter for the hydration force	m	5.00E-11

Pore water specifications			
T	Absolute temperature	K	293.15
ε	Electronic permittivity of pore water	$C^2/(J \cdot m)$	7.083E-10

The parameters are determined from oedometer tests, swelling tests, triaxial compression tests laboratory tests (Sasakura et al., 2002). In the next section, simulations of the basic behaviors of expansive soil are presented, and the basic parameters of the model are determined by fitting with observed results.

3.2 Simulations of basic characteristics of expansive soil

3.2.1 Soil water characteristics

Firstly, the parameters for the soil water characteristic were determined by fitting the observed soil water characteristic curves (SWCC) at various densities. Figure 4 shows the observed and computed SWCCs. The computed results were obtained from the simulations of the wetting process under constant densities, namely simulations of swelling pressure tests. In the simulations, the initial state properties of the air-dried Kunigel-V1 specimen were as follows: the suction is 8000 kPa (relative humidity = 55%); the cation concentrations are Na^+ = 3000 mol/m^3, Ca^{2+} = 0.25 mol/m^3, K^+ = 1.0 mol/m^3 and Mg^{2+} = 0.25 mol/m^3; the stresses are isotropically 10 kPa. This initial state is the same in the following simulations. During wetting process, the suction was decreased to 0.1 kPa. However, changes in cation concentrations are unclear in the experiments because of dilution as well as migration, diffusion, and convection. In the simulations, the values decreased to the following: Na^+ = 80 mol/m^3, Ca^{2+} = 0.37 mol/m^3, K^+ = 0.21 mol/m^3 and Mg^{2+} = 0.14 mol/m^3, which correspond to those of the slurry specimen for simplicity.

Although the observed results indicate the density dependency, the parameters of the proposed model, that does not consider it, were set to represent the average SWCC characteristic. The states at the highest suction for the observed results were obtained under the air-dried condition. Nevertheless, the degree of saturation under this condition was approximately 20%. This indicates that almost all of the water is adsorbed into the expansive mineral crystal. As expressed in equation (2), the degree of saturation of the proposed model includes such adsorbed water as the interlaminar void ratio, which is fully saturated. Therefore, the initial interlaminar void ratio e_0^{il} could be evaluated to satisfy the initial degree of saturation under the air-dried condition.

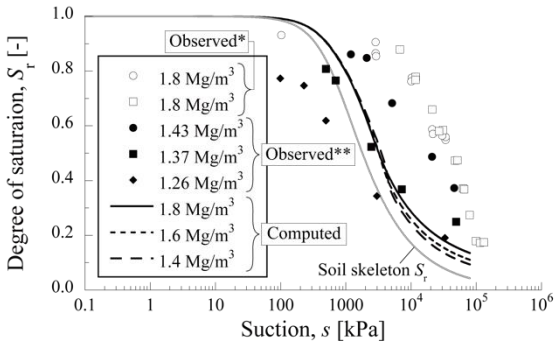


Figure 4. *Observed and computed soil water characteristic curves (* Suzuki and Fujita, 1999a; ** Ruan, 2022)*

3.2.2 Swelling of expansive mineral crystal

Almost bentonite specifications could be determined via X-ray diffraction measurements, concentration measurements, adsorption measurements, etc. However, only the parameters of the hydration force had to be investigated by fitting with the observed results. The simulation was conducted by decreasing the suction from the initial state at a constant molar ratio. Figure 5 shows the observed and computed results of the changes in the basal spacing (the interlaminar distance plus thickness of crystal) with relative humidity, which is converted from the suction.

As the relative humidity increases, the mineral crystals form a layered structure in the stepwise manner due to water adsorption (labeled 0 W, 1 W, 2 W, 3 W, and 4 W in Figure 5); thus, the basal spacings of the experiment expanded approximately 1.0, 1.26, 1.56, 1.86; and 2.16 nm (e.g., Saiyouri et al., 2000). On the other hand, the computed basal spacing continuously increased with relative humidity. In the model, this expansion is simulated as the combination of the hydration and osmotic forces, which continuously change with the degree of saturation. It is well known that the swelling in the interlayer

between approximately 1.0 and 2.2 nm (water molecule layers 1–4) is generally identified as crystalline swelling. When it expands beyond the hydration due to subsequent water uptake, osmotic swelling becomes dominant because the interlaminar space is sufficient for developing a diffusion double layer around the crystals (e.g., Yong, 1999).

Figure 6 shows the transition of repulsive hydration and osmotic pressures with the relative humidity in the model. At a lower relative humidity, the hydration force is dominant, and it decreases as

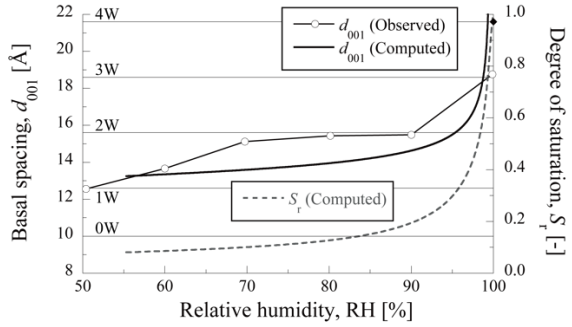


Figure 5. *Comparison of observed and computed changes in basal spacing with relative humidity*

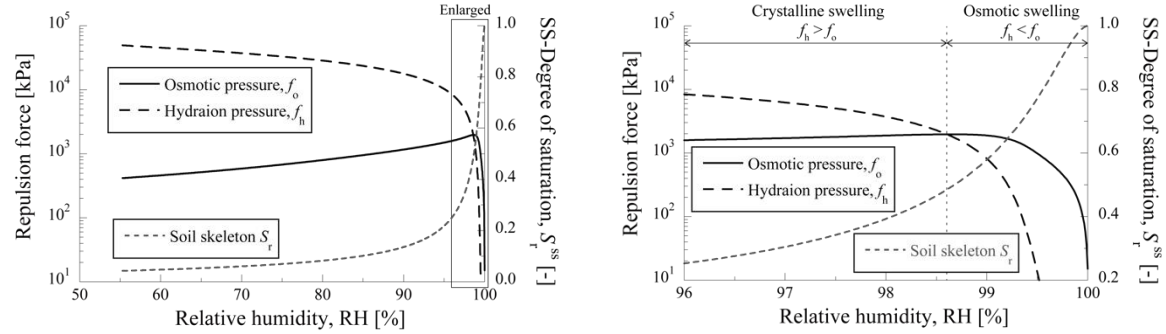


Figure 6. *Mechanism of microscopic swelling of expansive soil by the proposed model (left: entire, right: enlarged)*

swelling proceeds. Osmotic pressure gradually increases with relative humidity and becomes larger than the hydration force at the final stage of the wetting process. As a result of such transition of the hydration and osmotic pressures, the model can represent a continuous transition of the swelling of mineral crystal from initial crystalline swelling to osmotic swelling.

3.3 Simulation of swelling pressure tests

Simulations of swelling pressure tests at various densities were conducted. Overall, the time required to reach equilibrium of the swelling pressure test is shorter than that of the swelling deformation test under constant stress, in which an increase in the pore size would cause changes in permeability and cation concentrations. In other words, the cation concentrations may not change significantly during the swelling pressure test. Therefore, two series of simulations were conducted for the swelling pressure tests in this study. One was the swelling with a reduction in cation concentration, which is equivalent to that of the slurry specimen, as shown in Figure 4 in Section 3.2.1. The other is the swelling with a constant amount of substance, namely $S_{\mathrm{r}} e c_{\mathrm{i}}$ is constant.

Figure 7 shows a comparison between the observed swelling pressures and the computed results. Although the computed results are underestimated at higher densities, the proposed model can cover the observed swelling pressures over a wide range of densities. Moreover, the computed swelling pressures with a constant amount of substance is lower than those with a variable amount of substance at any densitiy. Unless any cations are added, the cation concentrations with a constant amount of substance would be higher. This indicates that the osmotic pressure with a constant amount of substance is the smallest, thus the swelling pressure is relatively small.

Figure 8 summarizes the transition of the state variables during the swelling pressure tests with a constant amount of substance: a) vertical stress (swelling pressure), b) degree of saturation, c) the interlaminar distance, and d) the soil skeleton void ratio. The degree of saturations continuously increases at any densities, followed by the expansion of the interlaminar distance. On the other hand, the vertical stresses initially increase but decrease at the intermediate wetting stage. Subsequently it increases again, and finally reach to equilibrium. This type of drop in swelling pressure has been observed in previous experimental studies (e.g., Zhu et al., 2013 and Wang, 2022). However, the soil skeleton void ratios decrease monotonically, and their reductions are significant in the cases of lower densities. These decreases in the soil skeleton void ratio are attributed to wetting collapse in the model. As the degree of saturation increases, the state variable ψ controlling the vertical position of the NCL, moves downward causing the collapse of the soil skeleton. Therefore, the expansion of the interlaminar distance is absorbed by the volume contraction of the soil skeleton.

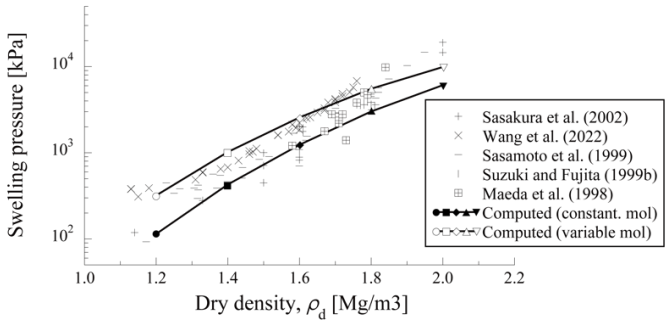
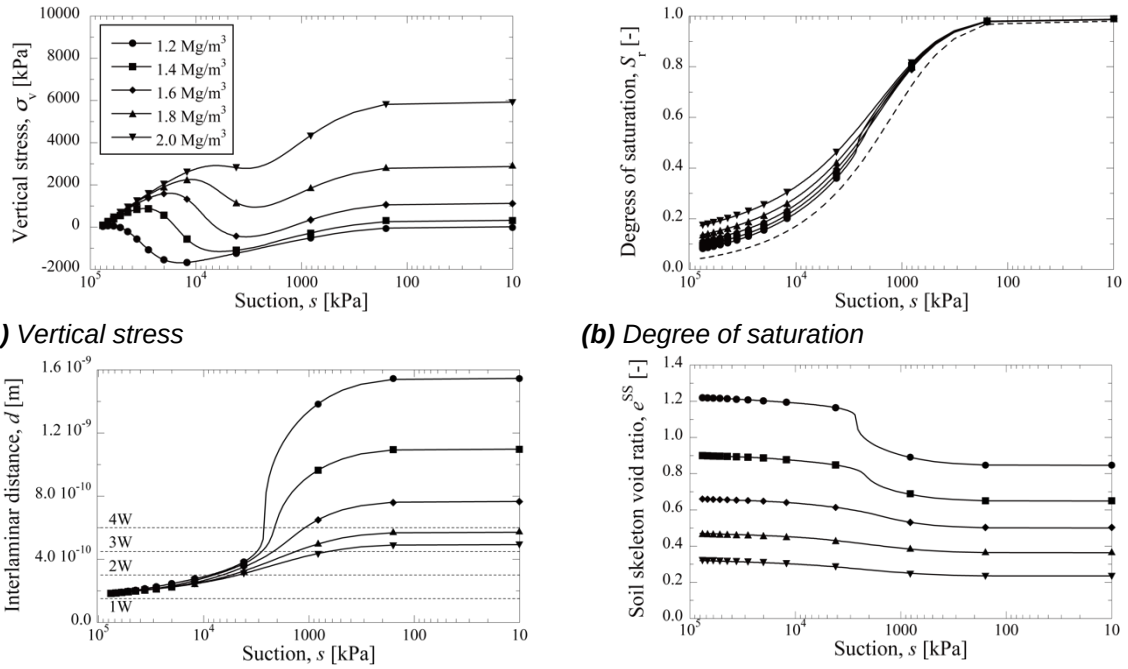


Figure 7. *Observed and computed results of swelling pressure tests at various densities*



(a) *Vertical stress* ***(b)*** *Degree of saturation*

(c) *Interlaminar distance* ***(d)*** *Soil skeleton void ratio*

Figure 8. *Transition of state variables during swelling pressure tests*

The simulation of swelling test was conducted by constraining the strain during the wetting process. Therefore, the vertical stress has a negative value (the tension stress state) in the case of a decreased density, in which the contraction of the soil skeleton is relatively larger than the interlaminar expansion. In a laboratory test, this situation corresponds to the top of the specimen being detached from the pressure plate of the apparatus, and it would actually occur or might have occurred. To appropriately describe this phenomenon, the swelling pressure test will be solved as a boundary value problem in future studies.

4 CONCLUSIONS

In this study, the constitutive model proposed by Kyokawa (2021) was extended to consider the multi-cation conditions. The influence of cation exchange on the osmotic pressure was considered as the adsorption ratio. The proposed model was applied to the wetting and swelling behaviors of the Kunigel-V1 bentonite. The model described a continuous swelling of mineral crystals from the crystalline swelling in the dry state to the osmotic swelling in the wet state, owing to the transition of the hydration and osmotic pressures. Moreover, the simulation of swelling pressure tests validated that the proposed model could reflect to the observed swelling pressures over a wide range of densities. The influence of cation concentrations on the swelling characteristics of bentonite is indicated. As a combination of the soil skeleton and the interlaminar behaviors, the proposed model could qualitatively evaluate the swelling pressure under various densities and their increase-decrease phenomena, as observed experimentally.

5 ACKNOWLEDGEMENTS

The authors would like to thank Dr. Ruan, Wased University, for providing the experimental data. This study was supported by JSPS KAKENHI Grant Number 22H01584.

REFERENCES

Alonso, E. E., Vaunat, J. and Gens, A. (1999). Modelling the mechanical behavior of expansive clays. Engineering Geology, 54, 173–183.

Gens, A. and Alonso, E.E. (1992). A framework for the behavior of unsaturated expansive clays. Canadian Geotechnical Journal 14, No. 1, 1013–1032.

Guimarães, L DO N., Gens, A., Sànchez, M. and Olivella, S. (2013). A chemo-mechanical constitutive model accounting for cation exchange in expansive clays, Géotechnique, 63, No. 3, 221–234.

Kikumoto, M., Kyokawa, H., Nakai, T. and Shahin, H. M. (2010). A simple elasto–plastic model for unsaturated soils and interpretations of collapse and compaction behaviours. Proceedings of the 5th International Conference on Unsaturated Soils (eds E. Alonso and A. Gens), Barcelona, 849–855.

Komine, H. and Ogata, N. (1996). Prediction for swelling characteristics of compacted bentonite. Canadian Geotechnical Journal 33, 11–22.

Komolvilas, V., Kikumoto, M. and Kyokawa, H. (2022). Mechanism of wetting–induced deformation and failure of unsaturated soils, International Journal for Numerical and Analytical Methods in Geomechanics, 46(6), pp. 1064–1092.

Kyokawa, H. (2021). A double structure model for hydro-mechano-chemical behavior of expansive soils based on the surface phenomena of mineral crystals, Engineering Geology, Vol. 294.

Liu, M. D., Likitlersuang, S., Horpibulsuk, S., & Ngo, D. H. (2021). 1D Constitutive Model for Expansive Soils. International Journal of Geomechanics, 21(3).

Maeda M., Tanai, K., Ito, M., Mihara, M. and Tanaka, M. (1998). Mechanical properties of the Ca exchanged and Ca bentonite; Swelling pressure, hydraulic conductivity, compressive strength and elastic modulus, PNC Report (PNC TN8410 98-021).

Mašín, D. (2017). Coupled Thermohydromechanical Double-Structure Model for Expansive Soils. Journal of Engineering Mechanics 143, No. 9, 04017067.

Millard, A., Mokni, N., Barnichon, J. D., Thatcher, K. E., Bond, A. E., Fraser-Harris, A., Mc Dermott, C., Blaheta, R., Michalec, Z., Hasal, M., Nguyen, T. S., Nasir, O., Fedors, R., Yi, H. and Kolditz, O. (2016). Comparative modelling of laboratory experiments for the hydro-mechanical behavior of a compacted bentonite-sand mixture. Environmental Earth Sciences 75:1311.

Navarro, V., Cabrera, V., ... Torres-Serra, J., 2022. A new double-porosity macroscopic model of bentonite free swelling. Engineering Geology 305.

Rosone, M., & Ferrari, A. (2022). Role of Stress History on the Swelling–Shrinkage Behavior of Compacted Scaly Clay. International Journal of Geomechanics, 22(9).

Saiyouri, N., Hicher, P. Y., Tessier, D. (2000). Microstructural Approach and Transfer Water Modelling in Highly compacted Unsaturated Swelling Clays. Mechanics of Cohesive-frictional Materials 5, No. 1, 41–60.

Sasakura, T., Kuroyanagi, M. and Okamoto, M. (2002). Studies on mechanical behavior of bentonite for development of the constitutive model, JNC Report (JNC TJ8400 2002-025).

Sasamoto, H., Isogai, T., Kikuchi, H., Sato, H. and Svensson, D. (2017). Mineralogical, physical and chemical investigation of compacted Kunigel V1 bentonite in contact with a steel heater in the ABM test package 1 experiment, Äspö laboratory, Sweden. Clay Minerals. Vol.52, 127-141.

Sun, W., Liu, C., Yang, D., & Sun, D. (2022). Evaluation of hydro-mechano-chemical behaviour of bentonite-sand mixtures. Journal of Rock Mechanics and Geotechnical Engineering, 14(2), 637–652.

Suzuki, H. and Fujita, T. (1999a). Unsaturated hydraulic propoerty of buffer material, JNC Report (JNC TN8430 99-010).

Suzuki, H. and Fujita, T. (1999b). Unsaturated hydraulic propoerty of buffer material, JNC Report (JNC TN8400 99-038).

Sànchez, M., Gens, A., Villar, M. and Olivella, S. (2016). Fully coupled thermo-hydro-mechanical double porosity formulation for unsaturated soils, International Journal of Geomechanics 16, No. 6.

Tuttolomondo, A., Ferrari, A., Laloui, L., 2021. An extended generalized effective stress for active clays. Canadian Geotechnical Journal 58, 1627-1639.

van Genuchten, M. T. (1980). A closed form equation for predicting the hydraulic conductivity of unsaturated soil. Soil Science Society of America Journal 44, No. 5, 892–898.

Wang, H., Ruan, K., Harasaki, S. and Komine, H. (2022). Effects of specimen thickness on apparent swelling pressure evolution of compacted bentonite. Soils and Foundations. Vol.62, 101099.

Yin, P., and Vanapalli, S. K. (2022). Model for predicting evolution of microstructural void ratio in compacted clayey soils. Canadian Geotechnical Journal, 59(9), 1602–1621.

Yong, R. M. (1999). Soil suction and soil-water potentials in swelling clays in engineered clay barriers. Engineering Geology 54, 3–13.

Zhu, C-M., Ye, W-M., Chen, Y-G, Chen, B and Cui, Y-J. (2013). Influence of salt solutions on the swelling pressure and hydraulic conductivity of compacted GMZ01 bentonite. Engineering Geology 166, 74–80.